

The Scaled Effective Solvent Method for Predicting the Equilibrium Ensemble of Structures with Analysis of Thermodynamic Properties of Amorphous Polyethylene Glycol-Water Mixtures

Hyeyoung Shin^a, Tod A. Pascal^{ab}, William A. Goddard III^{abc}, and Hyungjun Kim^{a*}*

^aGraduate School of EEWS, Korea Advanced Institute of Technology (KAIST), Daejeon, Korea

^bMaterial and Process Simulation Center, California Institute of Technology, Pasadena, CA 91125

^cWorld Class University Professor, KAIST, Daejeon, Korea

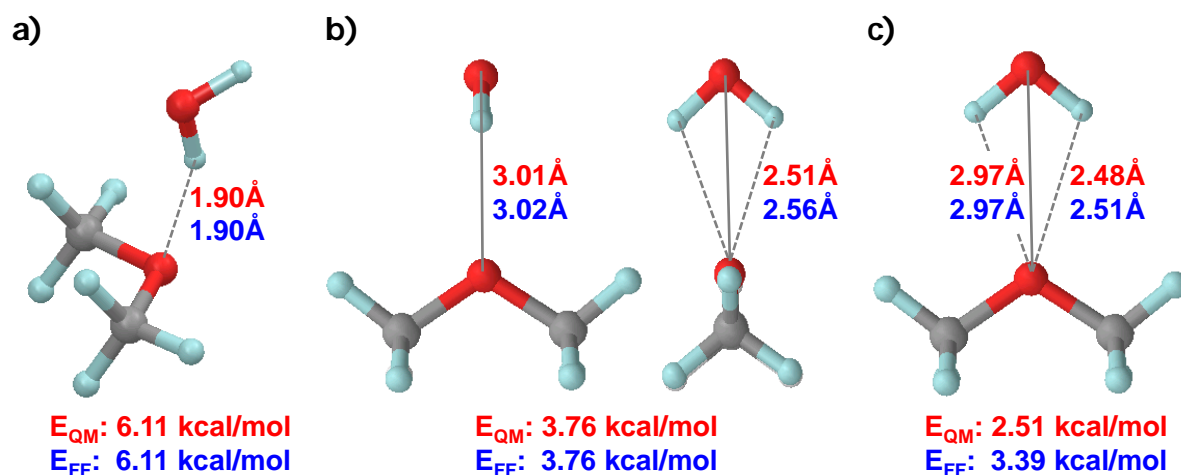


Figure S1. To describe the interaction between Polyethylene glycol (PEG) and water, we carried out quantum mechanical (QM) calculations using the M06-2X flavor of DFT with the cc-PVTZ++ basis set. We considered three types of optimized dimer structures between dimethyl ether (DME) and a water molecule from a) global minimum configuration, b) and c) structures optimized while constraining the point group symmetry of C_{2v} . QM calculation results and force field (FF) calculation results are described as red and blue fonts, respectively. Carbon atoms are gray-colored, oxygen atoms are red-colored, and hydrogen atoms are light blue-colored.

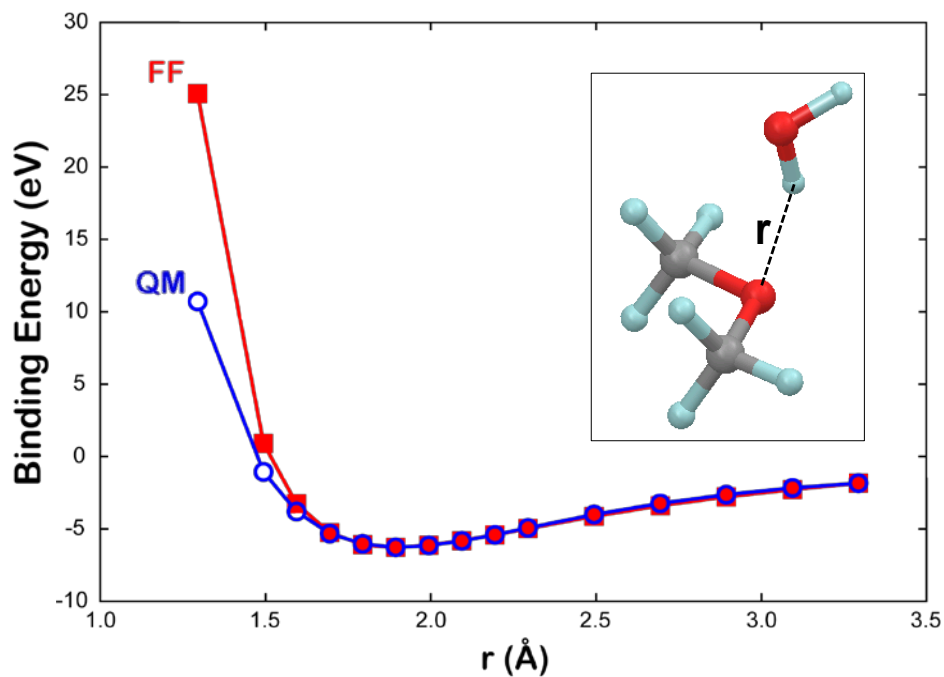


Figure S2. Dispersion curve obtained using the global minimum configuration (inset, Fig. S1a). Red solid line is calculated with the force field (FF) while the blue solid line is obtained from quantum mechanics (QM) calculation using M06-2X flavor of density functional theory (DFT) with the cc-PVTZ++ basis set. Carbon atoms are gray-colored, oxygen atoms are red-colored, and hydrogen atoms are light blue-colored.

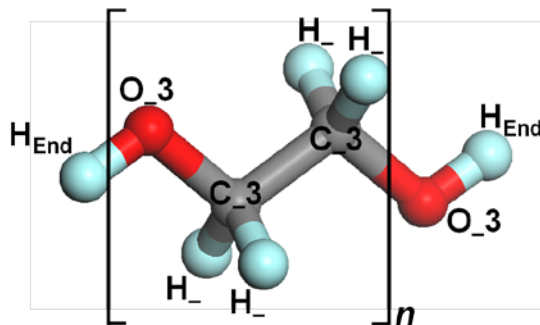
Table S1. In our simulations all force field parameters are DREIDING except that a) Van der Waal's (vdW) interactions between ether oxygen in a PEG backbone (O_{PEG}) and hydrogen in water (H_{wat}) are described with Morse potential [eq. (1)] and b) the explicit hydrogen bonding interactions are described by DREIDING hydrogen bond (H-bond) parameters above with the standard $(\cos \theta_{\text{OHO}})^4$ angular dependence and a cutoff at $\theta_{\text{OHO}}=90^\circ$ [12-10 Lennard-Jones (LJ) potential, eq. (2)]. We optimized off-diagonal vdW parameters first to reproduce the geometry and binding energy of dimethyl ether (DME) and water interaction imposing C_{2v} symmetry (Fig. S1b and S1c) where the explicit H-bond term has no contribution due to the angle cutoff. Then, we optimized the explicit H-bond term to reproduce the geometry and binding energy of the fully relaxed structure of DME and water (Fig. S1a).

$O_{\text{PEG}}\text{-}H_{\text{wat}}$	Van der Waals (Morse)			Hydrogen bond (12-10 LJ)	
	D_0 (kcal/mol)	R_0 (Å)	α	D_0 (kcal/mol)	R_0 (Å)
	0.3100	2.867	6.300	1.967	2.850

$$\text{Morse potential: } U(R) = D_0 \left\{ \left(\exp \left(- \left(\frac{\alpha}{2} \right) \left(\frac{R}{R_0} - 1 \right) \right) \right)^2 - 2 \exp \left(- \left(\frac{\alpha}{2} \right) \left(\frac{R}{R_0} - 1 \right) \right) \right\} \quad (1)$$

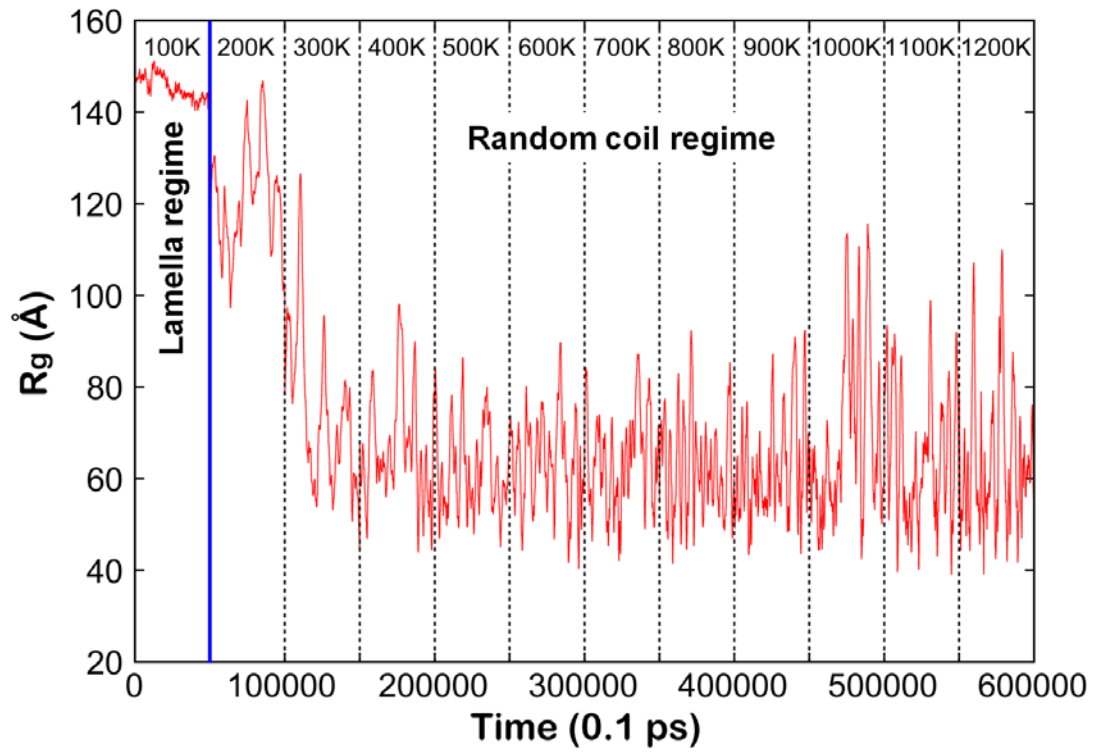
$$\text{12-10 LJ potential: } U(R) = D_0 \left\{ 5 \left(\frac{R_0}{R} \right)^{12} - 6 \left(\frac{R_0}{R} \right)^{10} \right\} \cos^4 \theta \quad (2)$$

Table S2. The partial charge distributions (q) of a 1,2-Ethandiol which represents the PEG model with a repeating unit ($n=1$) and a PEG-20kDa molecule with 455 repeating units ($n=455$). H_{End} is a hydrogen atom at both end sites of the PEG molecule. The partial charges for the 1,2-Ethandiol are electrostatic potential (ESP) charges derived from QM calculation with M06-2X/cc-PVTZ++ level and the partial charges of the PEG-20kDa are determined by modifying the partial charges of the 1,2-Ethandiol.

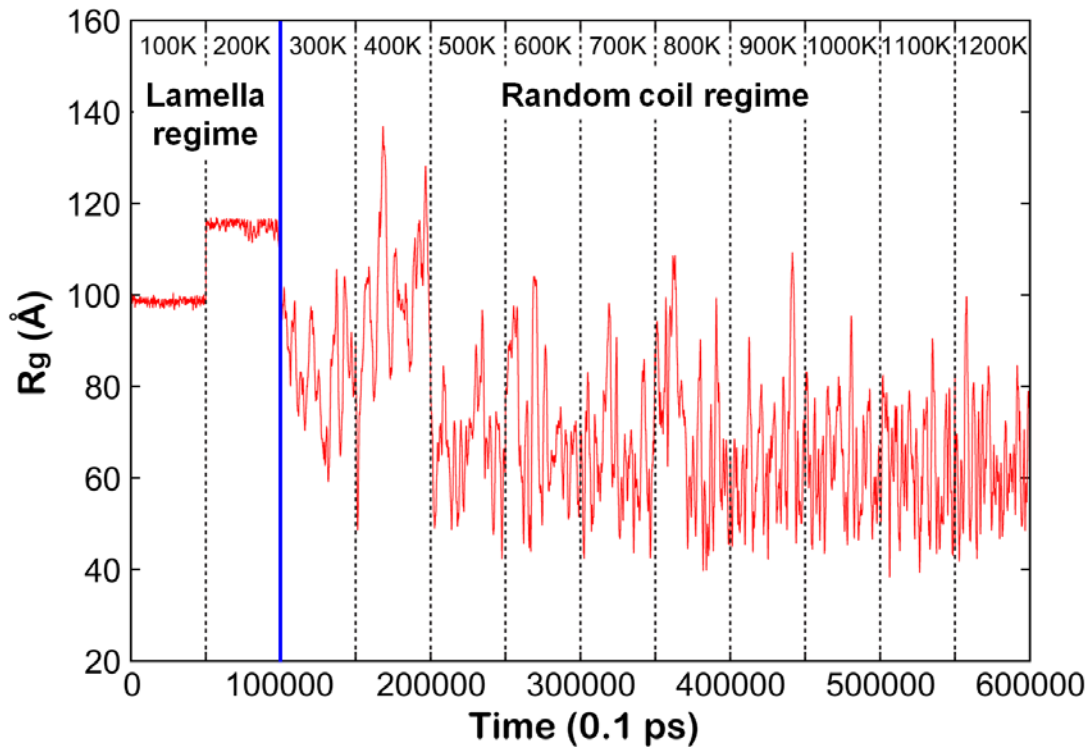


	1,2-Ethandiol ($n=1$)	PEG-20kDa ($n=455$)
H_{End}	0.00069	0.03699
O_3	-0.68317	-0.72384
C_3	0.28028	0.28765
H_{End}	0.40151	0.49387

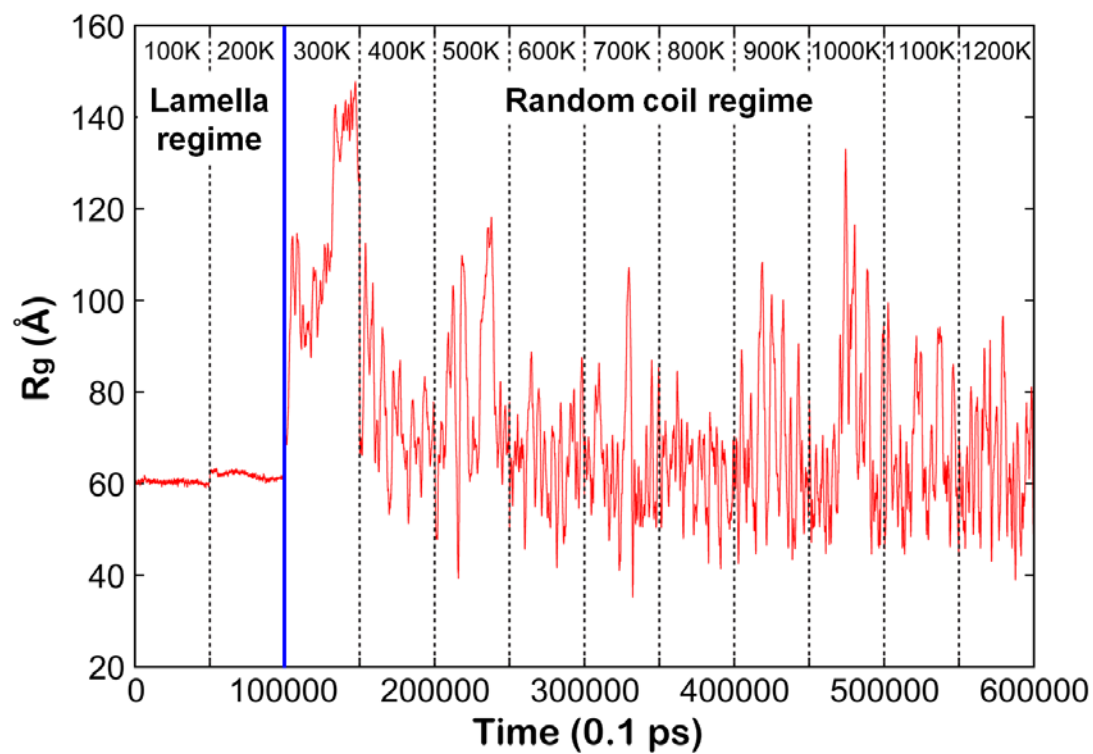
a) 0.1f



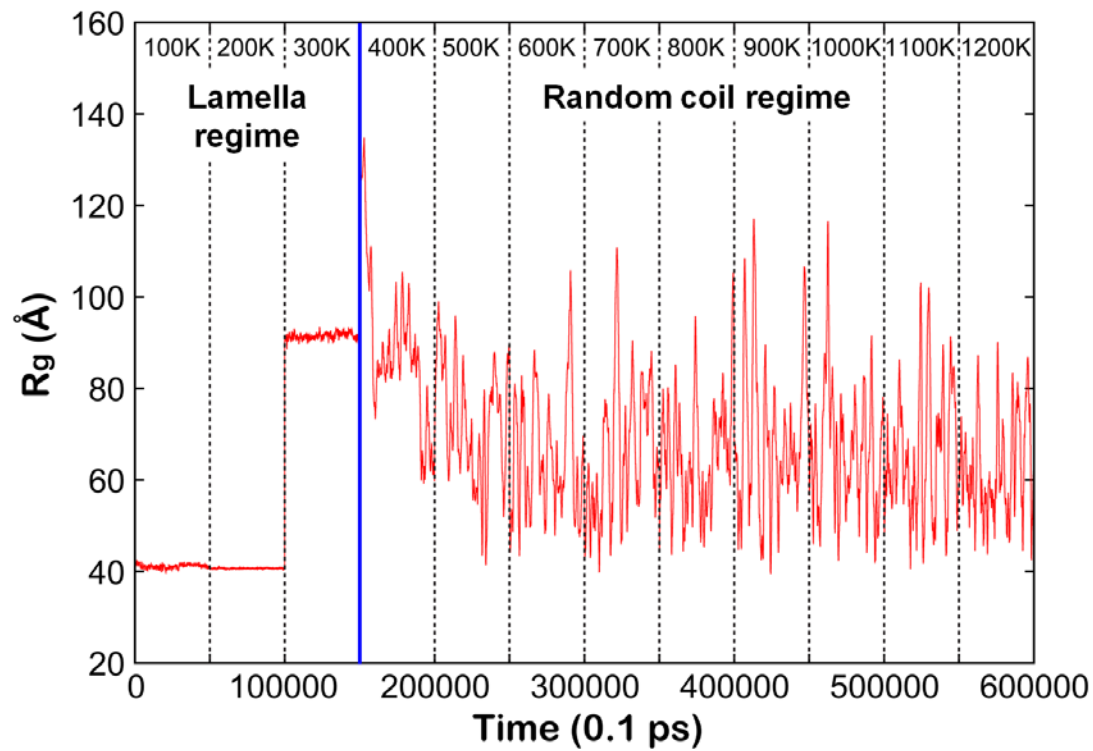
b) 0.2f



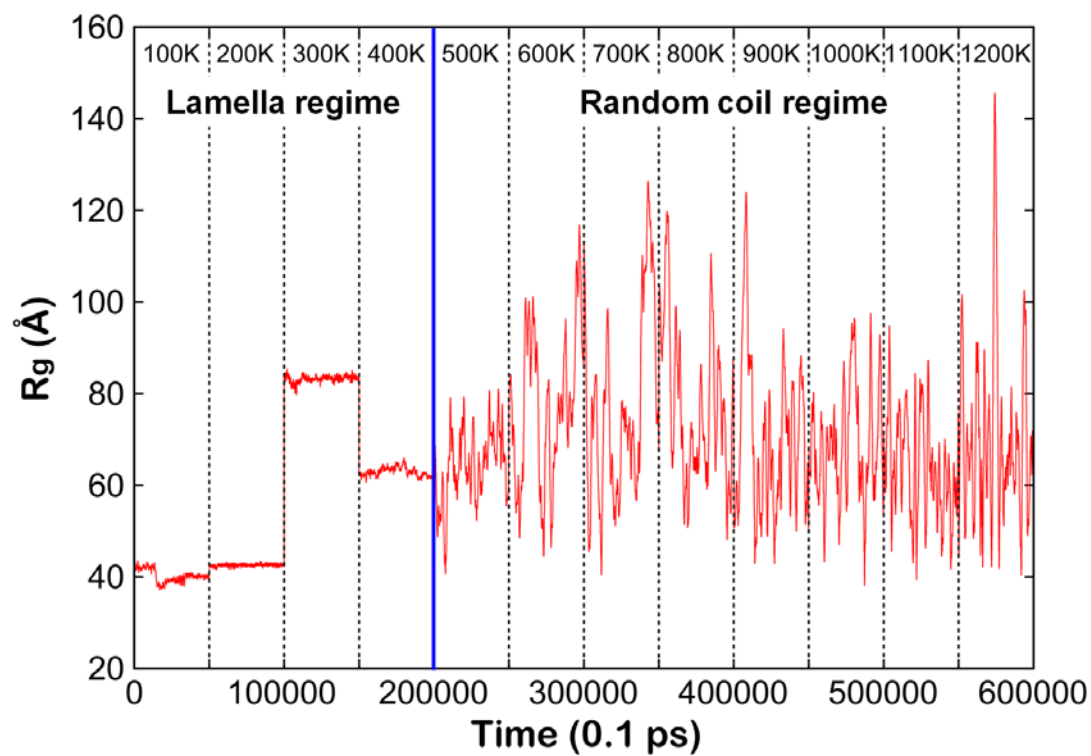
c) 0.3f



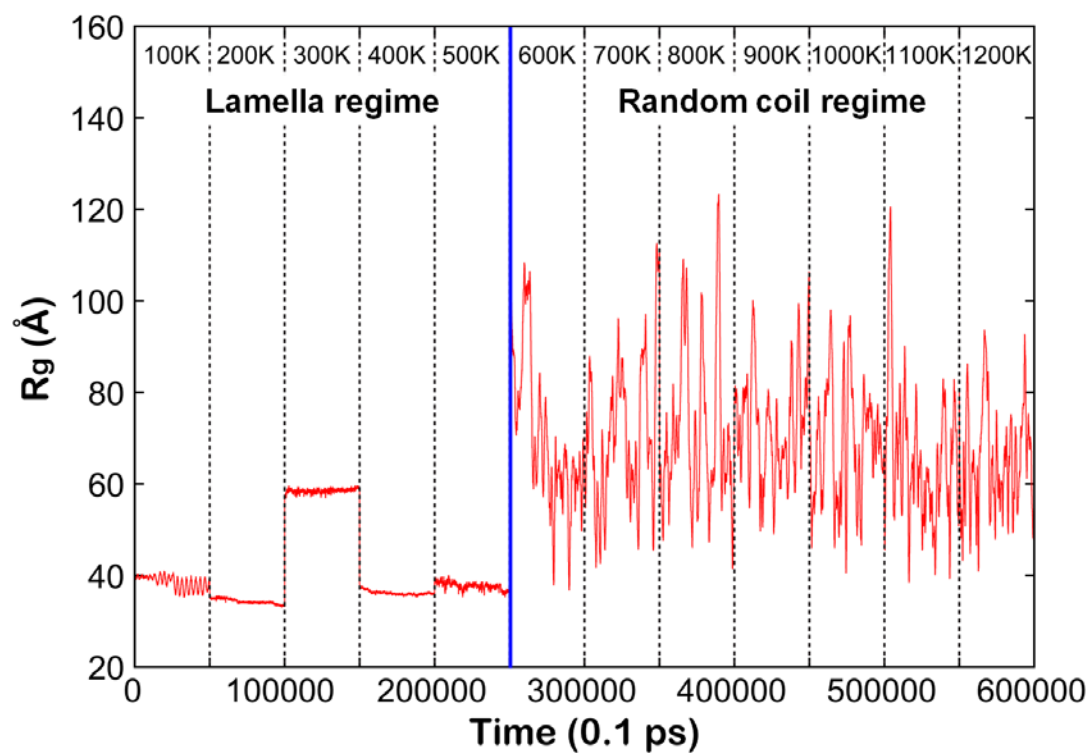
d) 0.4f



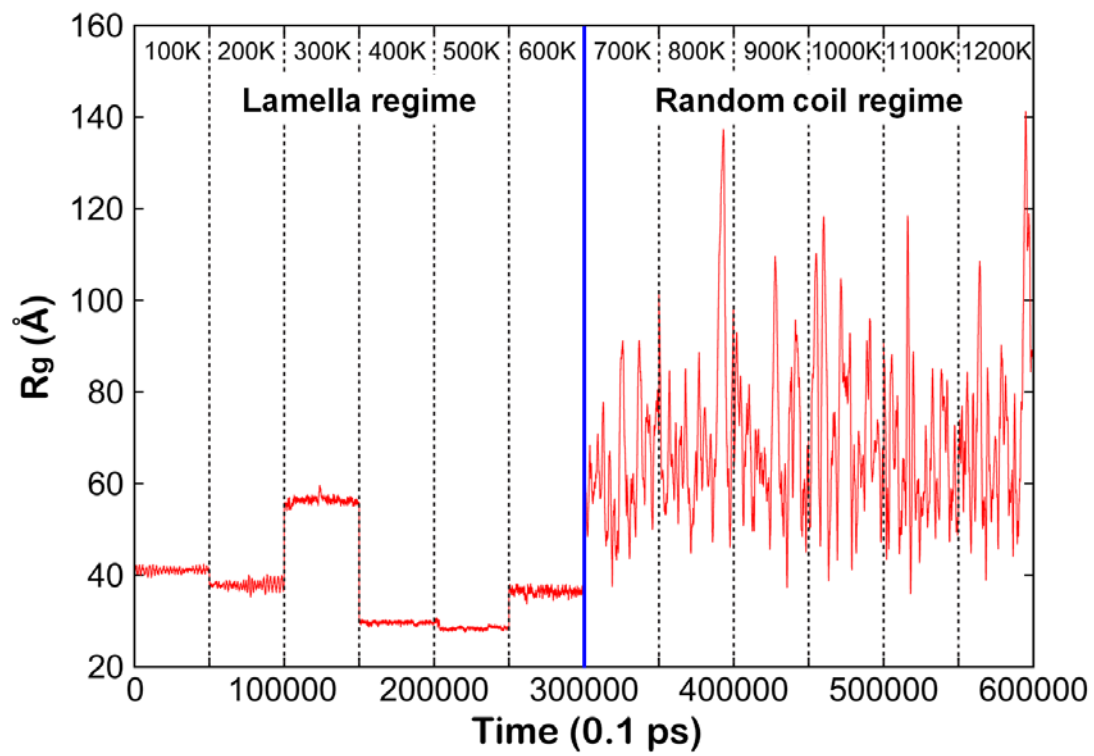
e) 0.5f



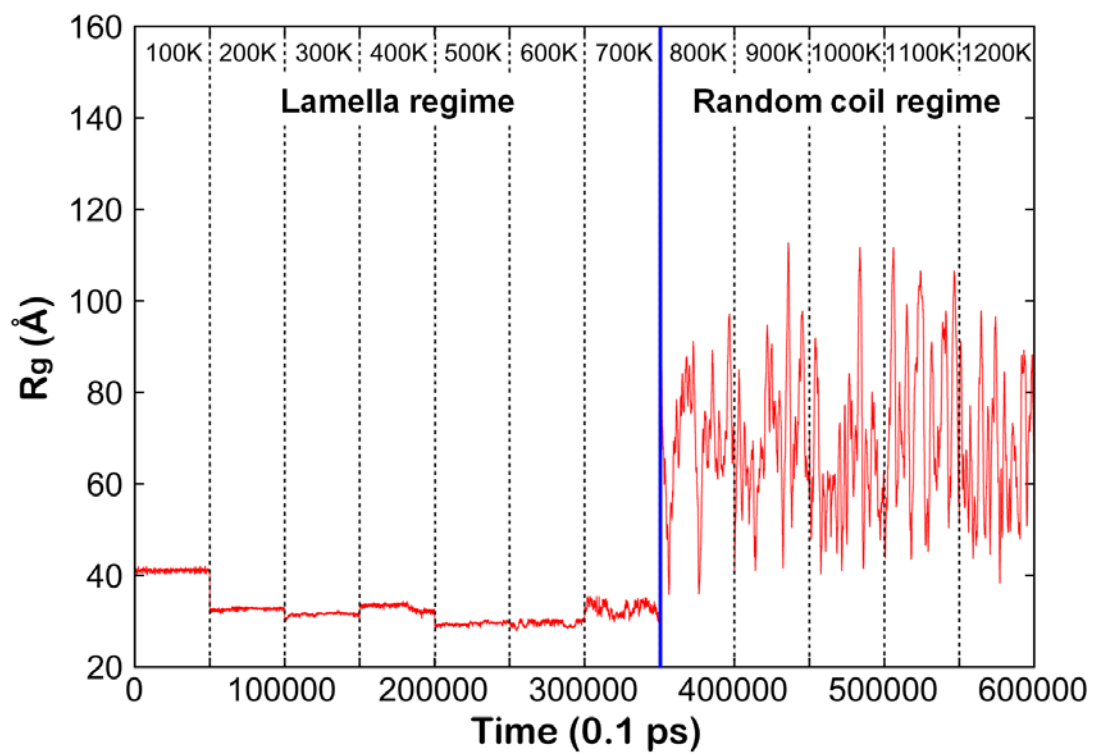
f) 0.6f



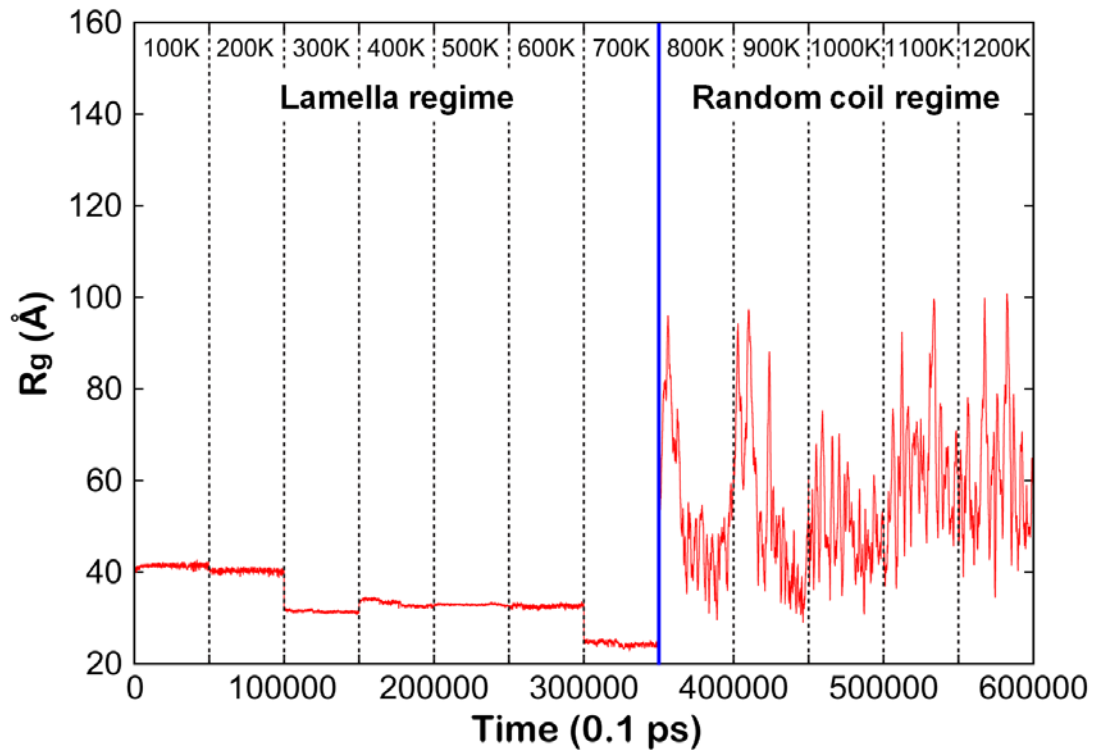
g) 0.7f



h) 0.8f



i) 0.9f



j) 1.0f

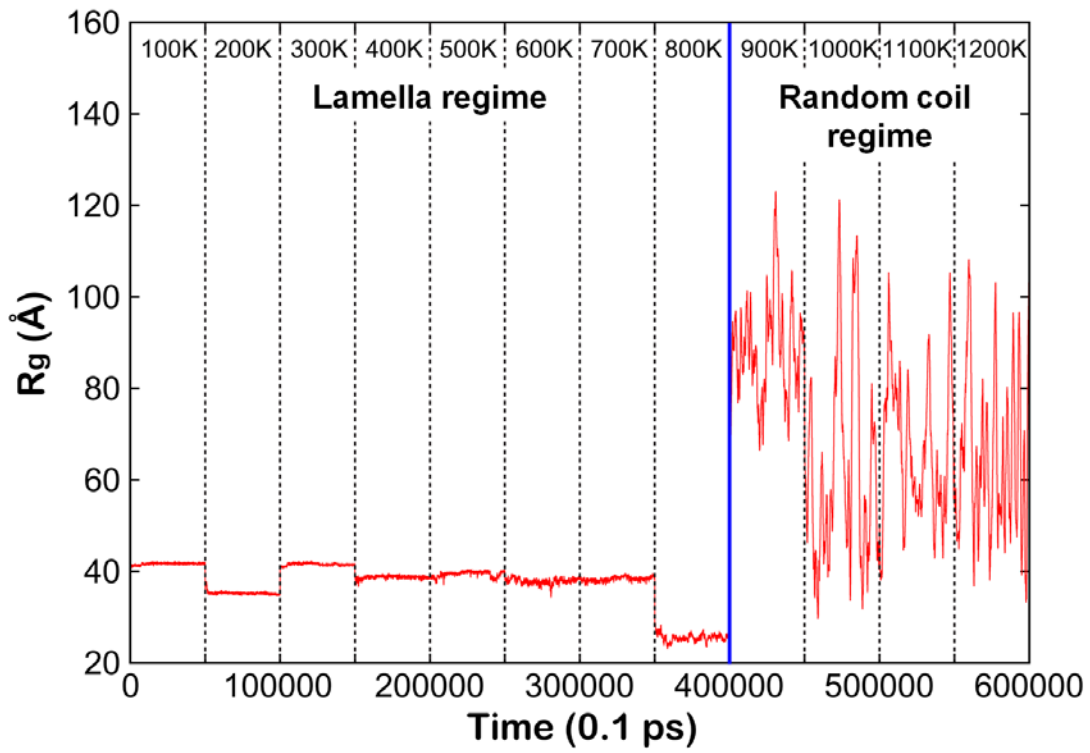


Figure S3. R_g variation with time during individual last 5ns NVT dynamics using scaling factor, f ; a) $f=0.1$, b) $f=0.2$, c) $f=0.3$, d) $f=0.4$, e) $f=0.5$, f) $f=0.6$, g) $f=0.7$, h) $f=0.8$, i) $f=0.9$, and j) $f=1.0$ for each temperature ranging from 100 K to 1200 K. On the left side of blue solid line, R_g values change little with very small fluctuation while on the right side of the blue solid line the R_g fluctuates dramatically with time. This distinction arises because below the θ temperature the strong intra-chain interactions dominate leading lamellar structures while above the θ temperature, thermal effects dominate leading to random coil (R-coil) structures. Therefore, we distinguish these two regimes as lamella regime and R-coil regime separated by the θ temperature.

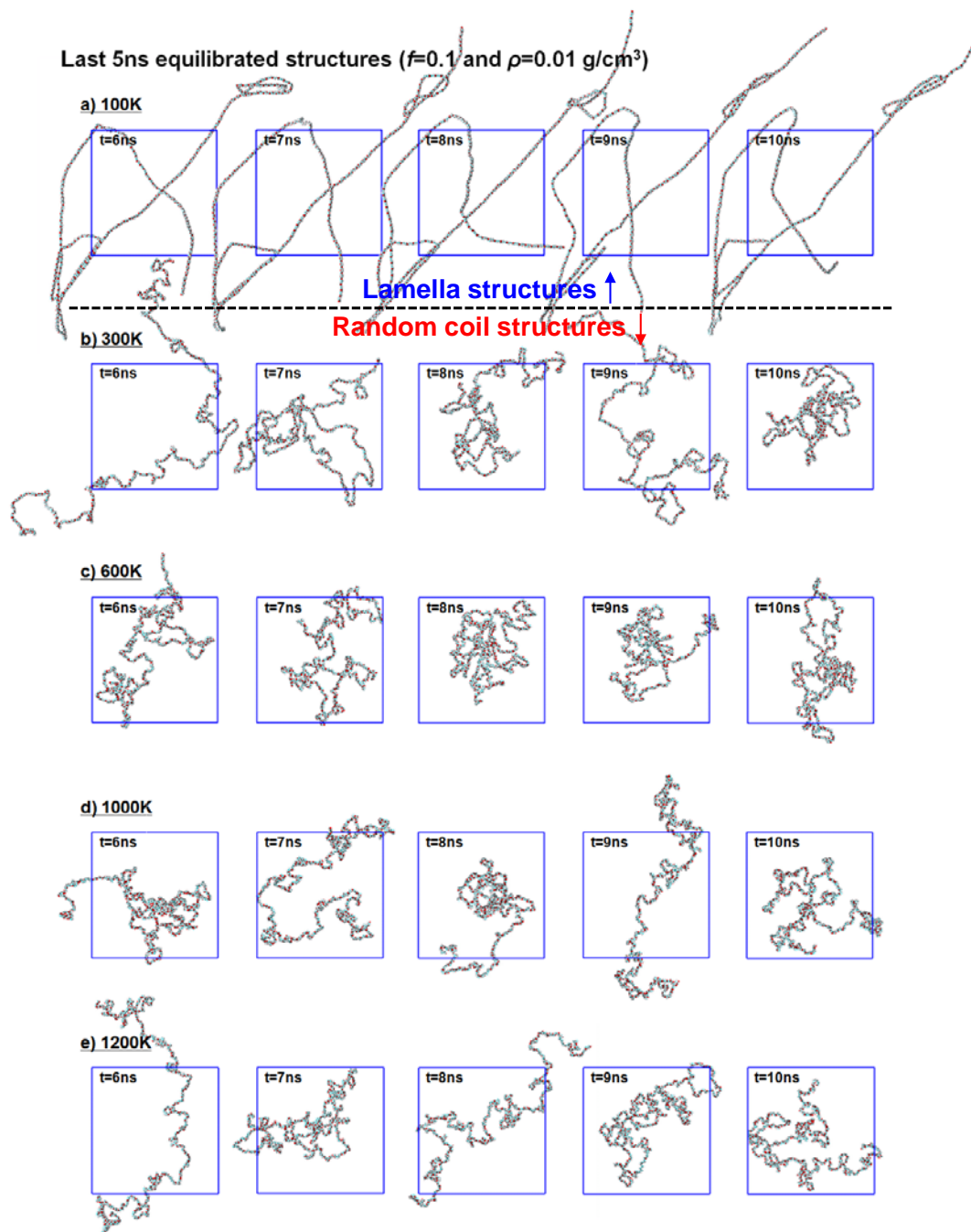


Figure S4. The $f=0.1$ scaled effective solvent (SES) case. Structures of a PEG-20kDa chain with $\rho=0.01$ g/cm³ sampled over the last 5ns NVT dynamics a) at $T=100$ K, b) at $T=300$ K, c) at $T=600$ K, d) at $T=1000$ K, and e) at $T=1200$ K. Over the temperature range from 200 K to 1200 K, the last 5ns of equilibrated PEG-20kDa conformations all show random coil like behavior in which the backbone of the polymer moves randomly in three-dimensional space, while at 100 K and below the PEG structures maintain a lamellar shape. White, red and green atoms are hydrogen, oxygen and carbon atoms respectively. The periodic box is shown as a blue solid line.

Last 5ns equilibrated structures ($f=0.5$ and $\rho=0.01$ g/cm³)

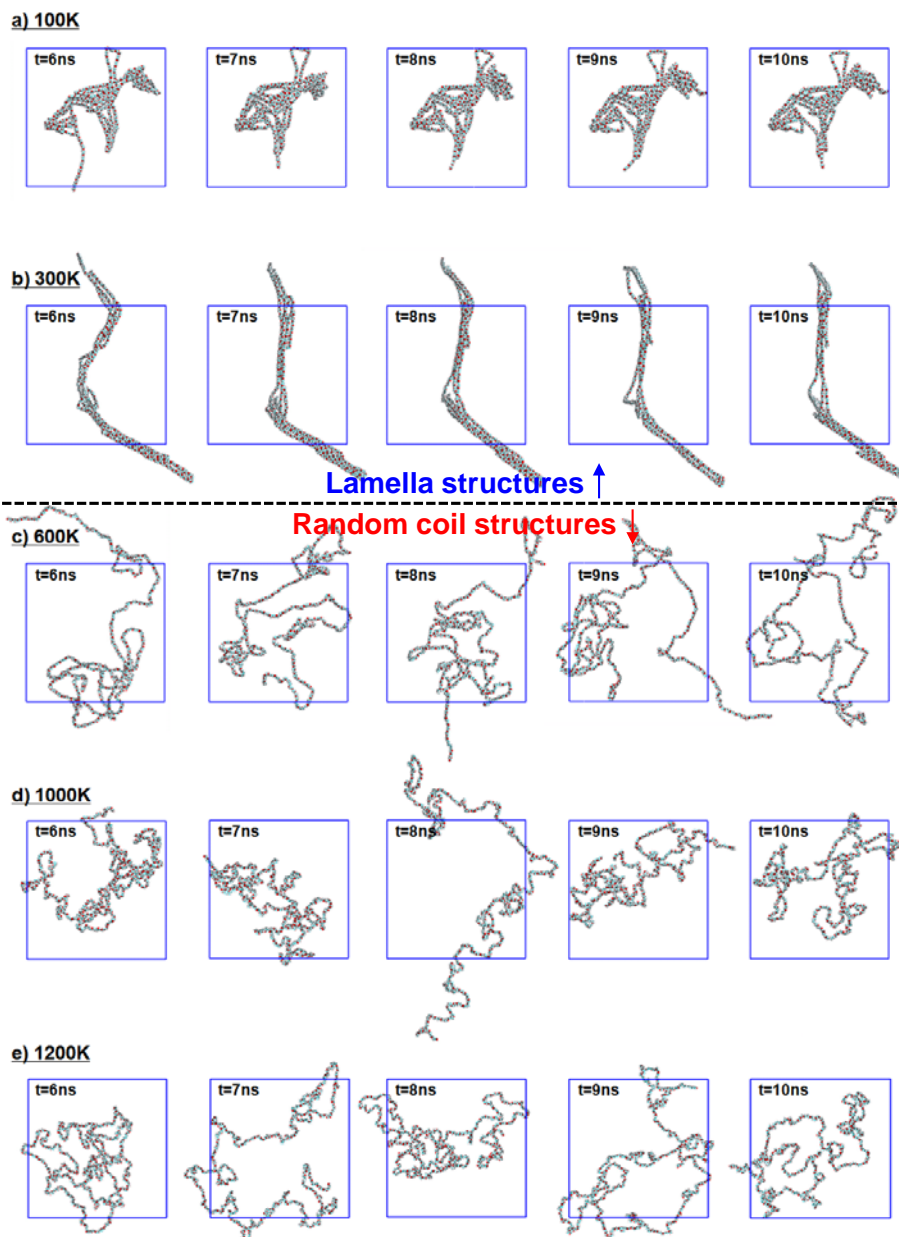


Figure S5. The $f=0.5$ scaled effective solvent (SES) case. Structures of a PEG-20kDa chain with $\rho=0.01$ g/cm³ sampled over the last 5ns NVT dynamics a) at $T=100$ K, b) at $T=300$ K, c) at $T=600$ K, d) at $T=1000$ K, and e) at $T=1200$ K. Over the temperature range from 500 K to 1200 K, the last 5ns of equilibrated PEG-20kDa conformations all show random coil like behavior in which the backbone of the polymer moves randomly in three-dimensional space, while at 400 K and below the PEG structures maintain a lamellar shape. White, red and green atoms are hydrogen, oxygen and carbon atoms respectively. The periodic box is shown as a blue solid line.

Last 5ns equilibrated structures ($f=0.7$ and $\rho=0.01$ g/cm³)

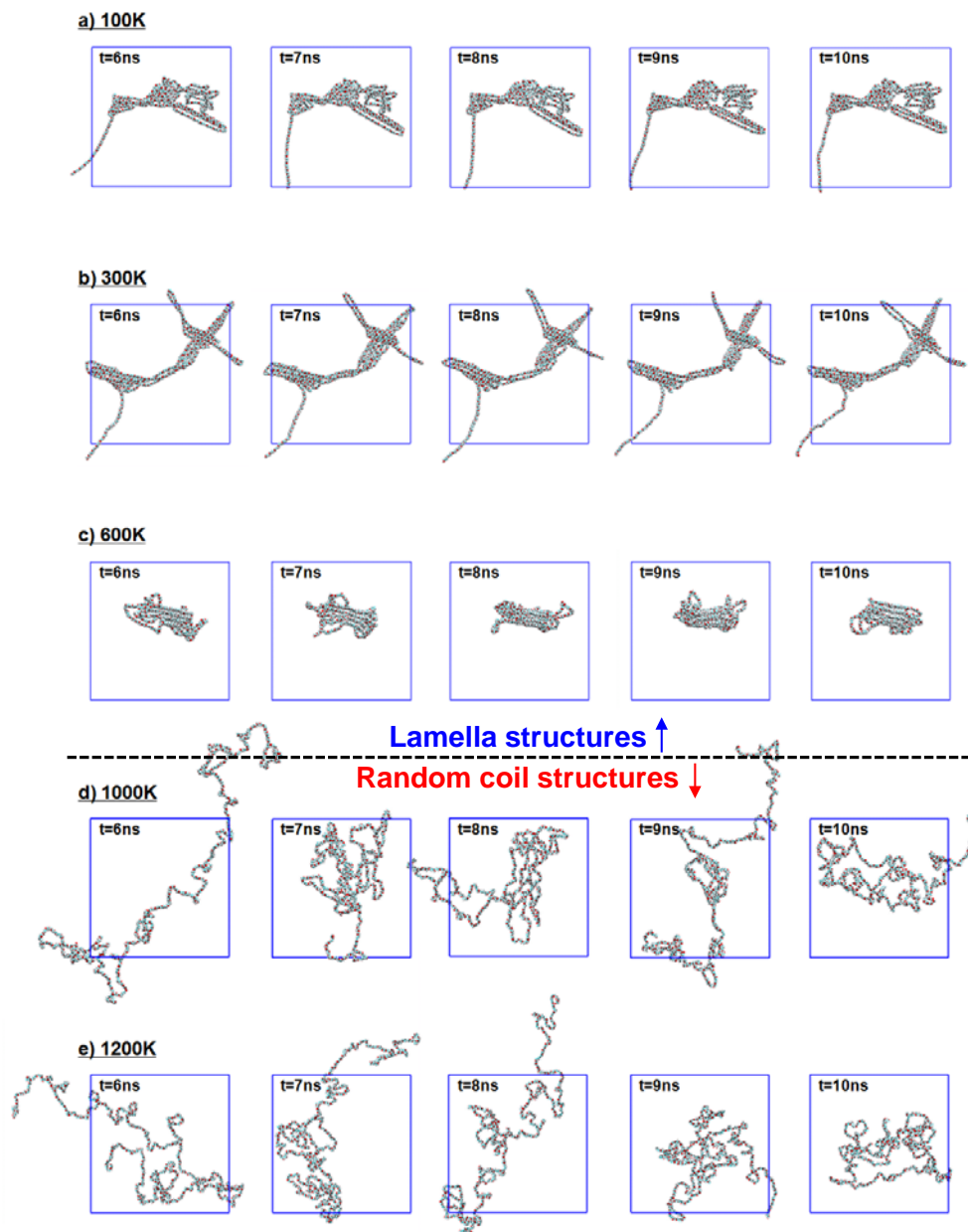
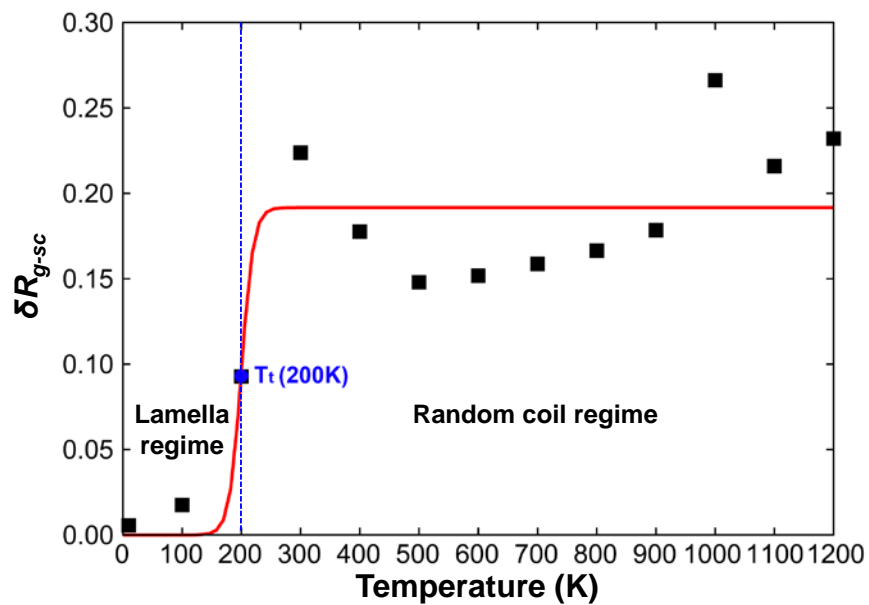
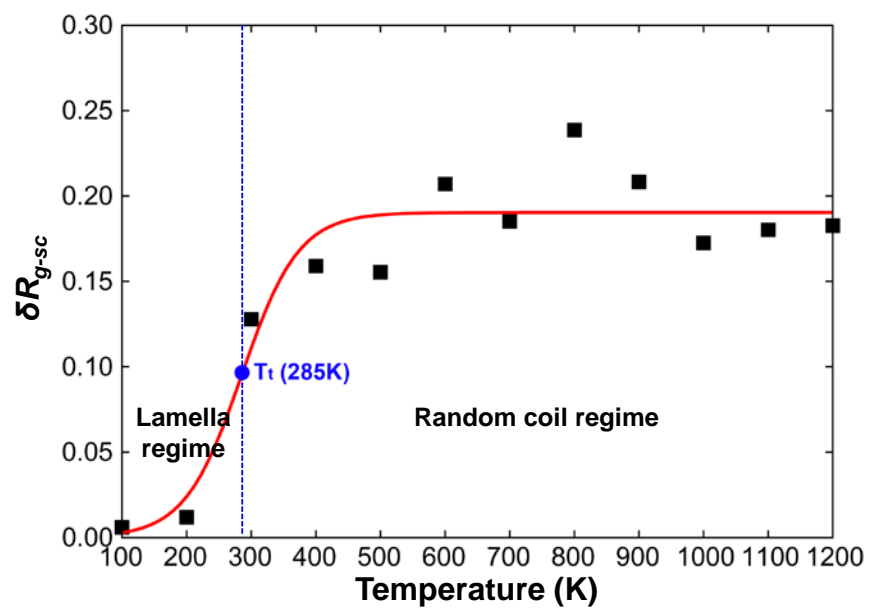


Figure S6. The $f=0.7$ scaled effective solvent (SES) case. Structures of a PEG-20kDa chain with $\rho=0.01$ g/cm³ sampled over the last 5ns NVT dynamics a) at $T=100$ K, b) at $T=300$ K, c) at $T=600$ K, d) at $T=1000$ K, and e) at $T=1200$ K. Over the temperature range from 700 K to 1200 K, the last 5ns of equilibrated PEG-20kDa conformations all show random coil like behavior in which the backbone of the polymer moves randomly in three-dimensional space, while at 600 K and below the PEG structures maintain a lamellar shape. White, red and green atoms are hydrogen, oxygen and carbon atoms respectively. The periodic box is shown as a blue solid line.

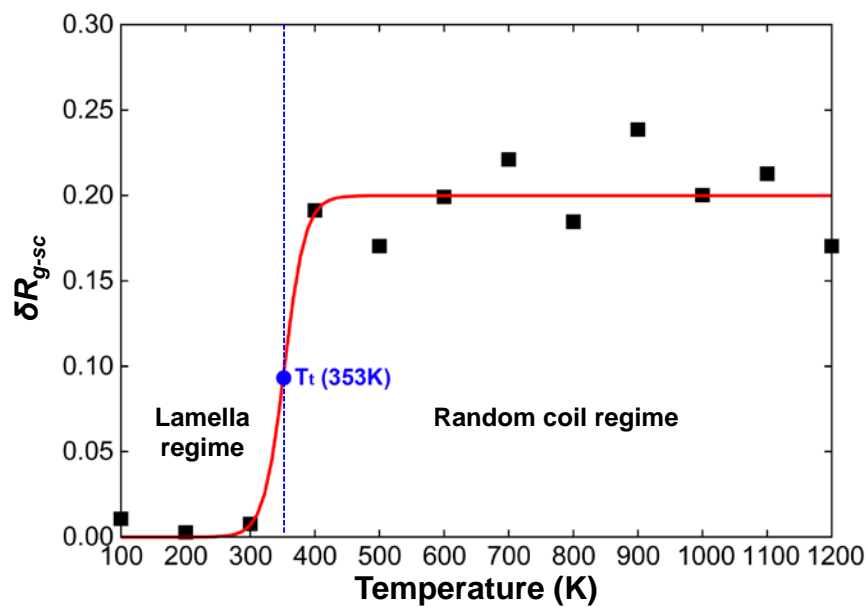
a) $f=0.1$



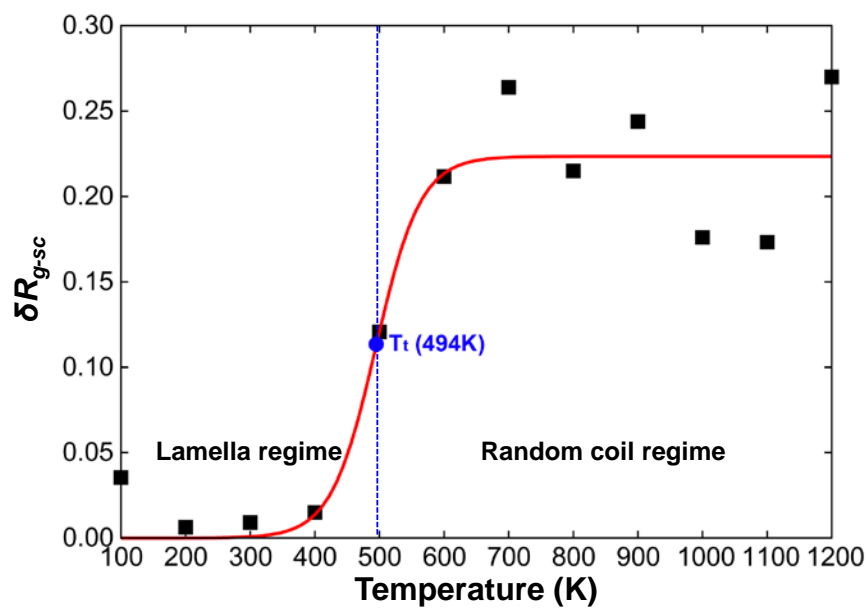
b) $f=0.2$



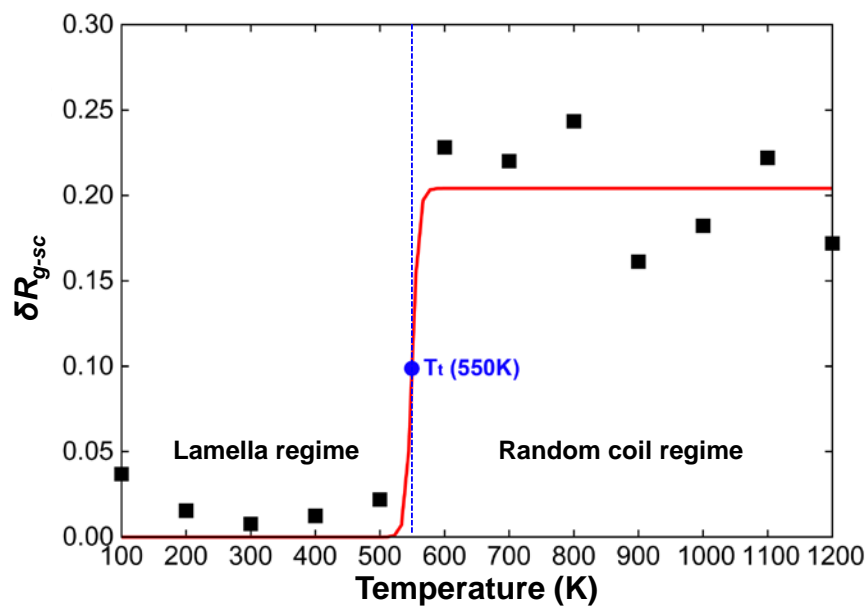
c) $f=0.4$



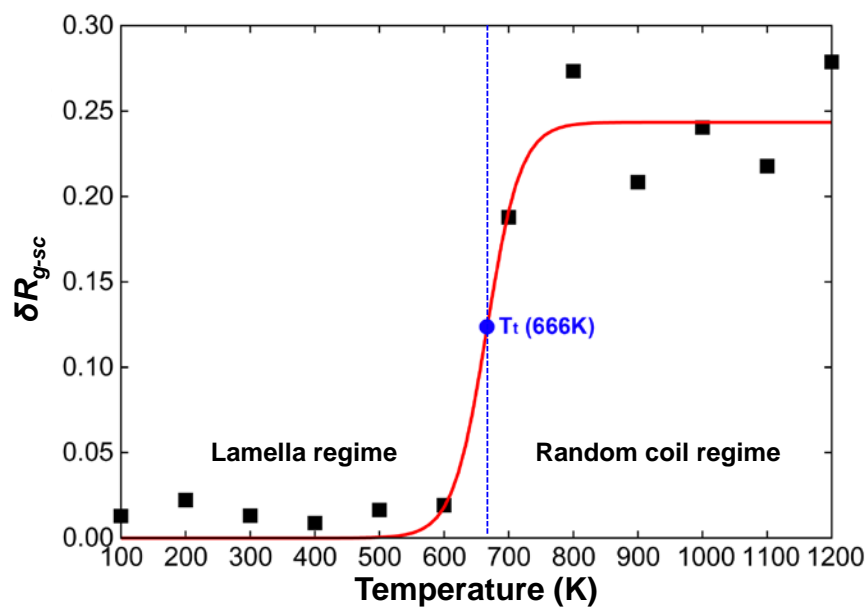
d) $f=0.5$



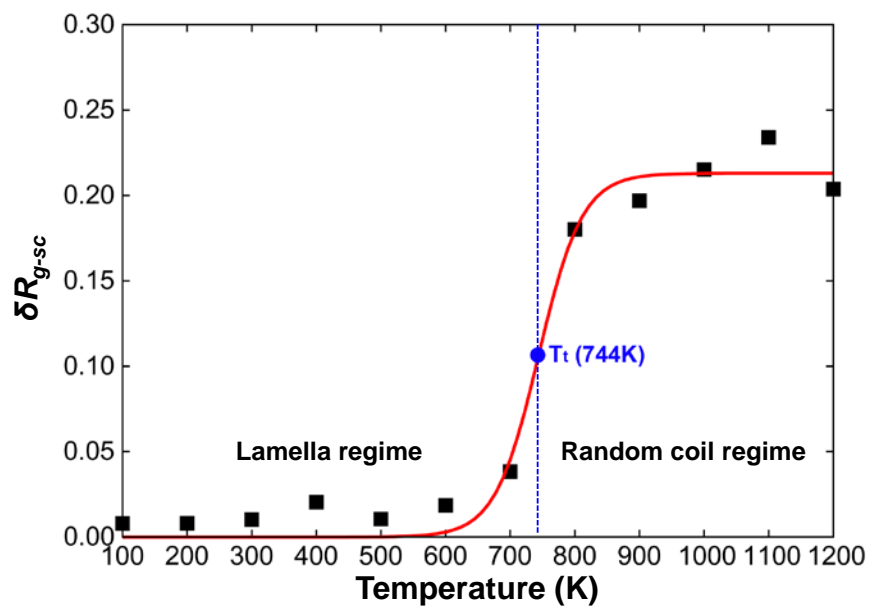
e) $f=0.6$



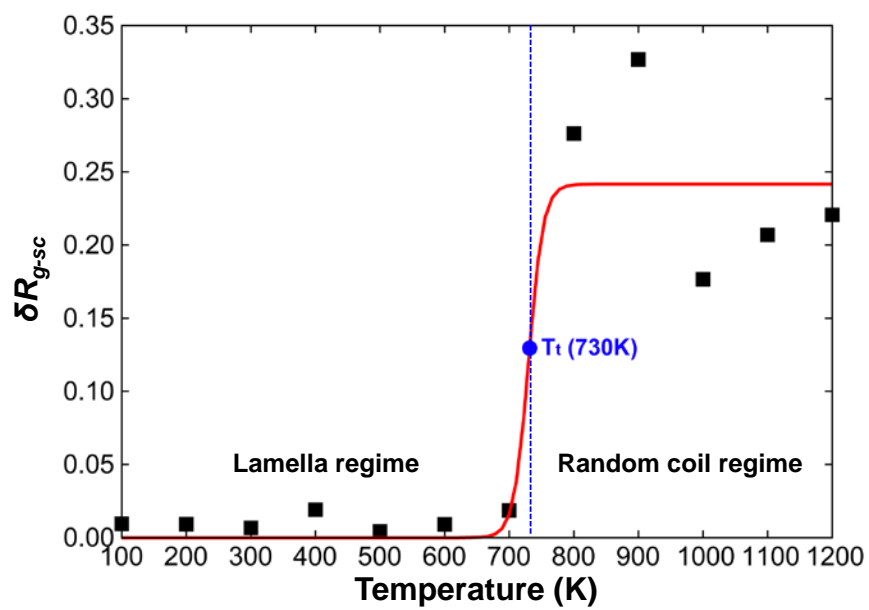
f) $f=0.7$



g) $f=0.8$



h) $f=0.9$



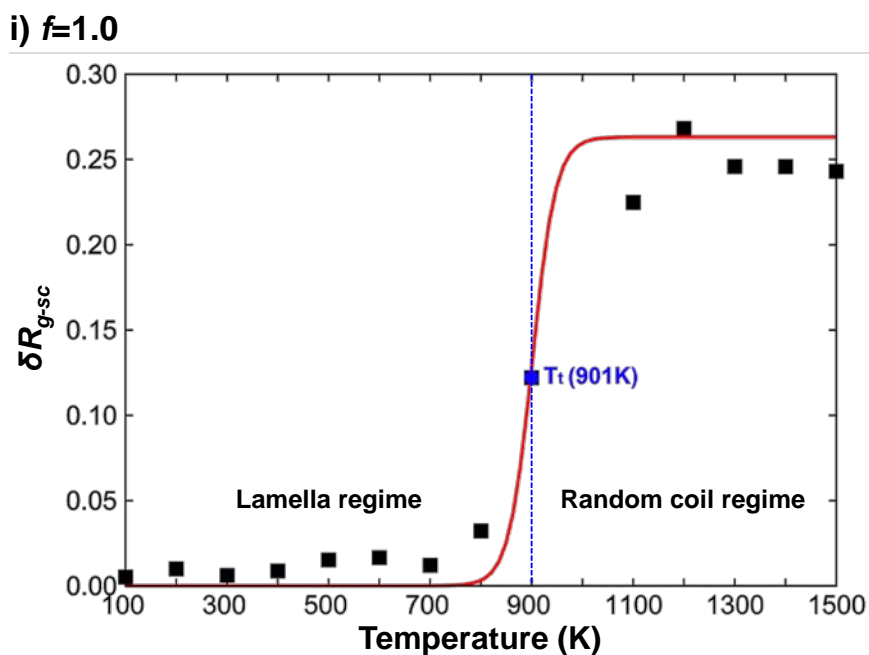


Figure S7. The scaled standard deviation of R_g , $\Delta R_{g-sc} = (\text{standard deviation of } R_g)/(\text{average } R_g)$, over the last 5ns NVT dynamics for each temperature ranging from 100 K to 1200 K (100 K to 1500 K for the case of $f=1.0$) using a large simulation cell with $\rho=0.01 \text{ g/cm}^3$ a) $f=0.1$, b) $f=0.2$, c) $f=0.4$, d) $f=0.5$, e) $f=0.6$, f) $f=0.7$, g) $f=0.8$, h) $f=0.9$, and i) $f=1.0$ For all values of f , we find a similar character that low temperature leads to a globular or lamella structures with small $\Delta R_{g-sc} (< \sim 0.04)$ and high temperature leads to a random coil (R-coil) structures with $\Delta R_{g-sc} > \sim 0.09$. At the highest temperature, the value of ΔR_{g-sc} is similar to the value expected for an infinite Gaussian coil, 0.26. To determine a precise θ temperature (T_t) to serve as the boundary between these two regimes, we used the hyperbolic tangent function, $\Delta R_{g-sc}(T) = a[\tanh\{(T - T_t)/b\} + 1]$, where T_t is indicated by blue circle point.

Table S3. At the highest temperatures (1200K), the scaled standard deviation of R_g , $\delta R_{g-sc} =$ (standard deviation of R_g)/(average R_g), calculated from the hyperbolic tangent function which was derived to determine the θ temperature as a function of the scaling factor, f .

f	0.1	0.2	0.3	0.4	0.5	0.6	0.7	0.8	0.9	1
δR_{g-sc}	0.192	0.190	0.198	0.200	0.223	0.204	0.243	0.213	0.242	0.263

Table S4. The scaled standard deviation of R_g , $\delta R_{g-sc} = (\text{standard deviation of } R_g)/(\text{average } R_g)$, for the ideal Gaussian chains with different number of monomers or polymer chains. We carried out stochastic simulation to generate number of polymers, N_{pol} , with the number of segments, n . The fluctuation of R_g is then numerically calculated, which is in turn determined as ~ 0.26 at the limit of N_{pol} and n are both infinity (regardless of the segmentation length). This compares well with the values we calculate above the transition temperature of $\delta R_{g-sc} = 0.19\text{--}0.26$ (see Table S3), validating that the polymer behaves like a random coil above the transition.

$N_{pol} \backslash n$	10	50	100	200	500	1000
100	0.231	0.263	0.254	0.257	0.255	0.253
1000	0.230	0.246	0.259	0.257	0.249	0.259
10000	0.227	0.255	0.262	0.259	0.255	0.261
100000	0.227	0.255	0.258	0.259	0.258	0.258
1000000	0.227	0.254	0.257	0.258	0.259	0.259

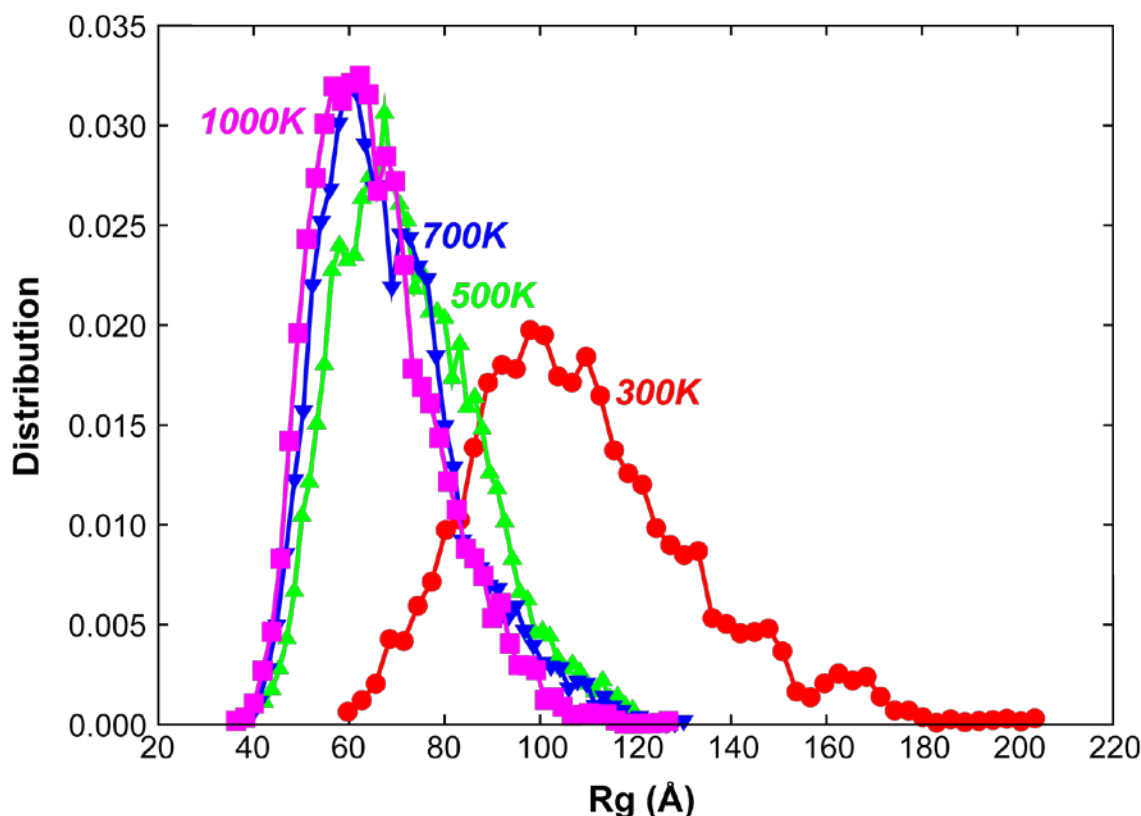


Figure S8. R_g distribution of random coils sampled with scaling factor of 0.3 as a function of temperature. The case of 300 K is red-colored, the case of 500 K is green-colored, the case of 700 K is blue colored, and the case of 1000 K is magenta-colored. For each temperature, R_g distribution of random coils is obtained from MD simulation for 110 ns.

In addition to the globule region we find two range of temperature.

1) Intermediate temperature range where there is nearly a balance between thermal effects and the scaled chain-chain interaction, but not sufficiently high to freely overcome the torsional barriers. This leads the sampling of random-coiled structures but biased to sample the expanded forms due to the stiffness of the polymer backbone, see for example the $T=300$ K case for $f=0.3$ (red solid line)

2) High temperature range where kT is high enough to freely overcome the torsional barriers, leading to bias toward more packed random-coiled conformations. See the $T=500$ K and above for the case with $f=0.3$

From the 2PT free energy analysis in the last part of our manuscript, sampling this full temperature range is important since all sampled conformations from all different temperatures have comparable free energy values after including solvation effect explicitly in full solvent 300 K dynamics.

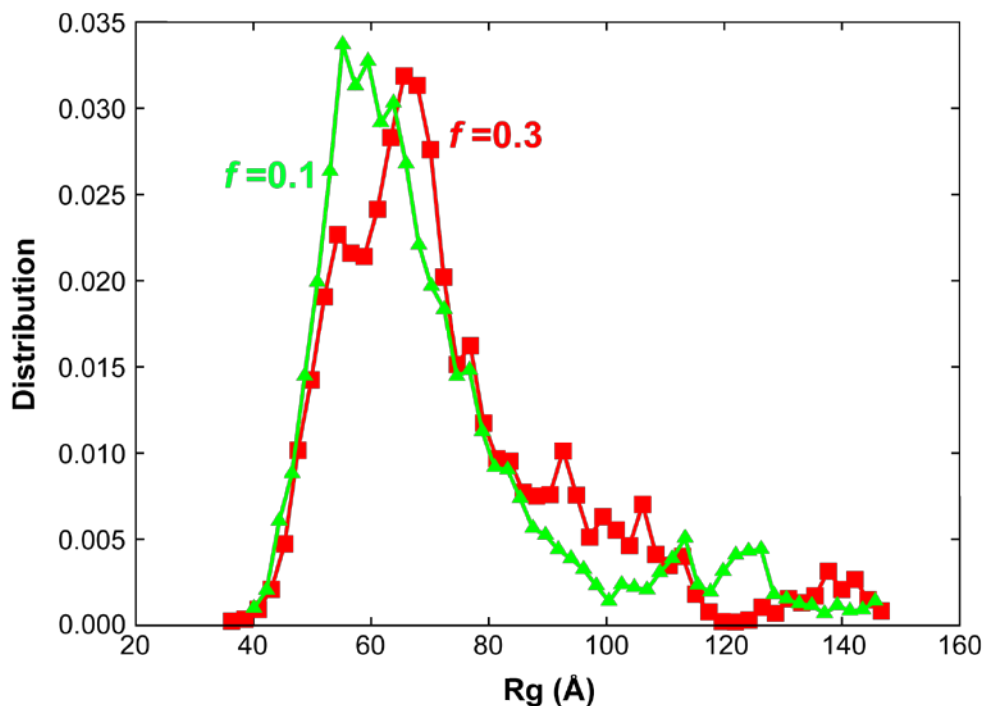


Figure S9. R_g distributions obtained by using $f=0.3$ (red) or 0.1 (green) and varying temperature in large simulation box ($140 \times 140 \times 140 \text{ \AA}^3$) with $\rho=0.01 \text{ g/cm}^3$. For all cases, we include all temperatures above the θ temperature (that is all temperatures for the R-coil structures from 100 K up to $\sim 1,200$ K).

This figure shows that the case of $f=0.1$ but varying the temperature up to $\sim 1,200$ K leads to a similar distribution to that of the case with $f=0.3$ with a similar $\Delta R_g \sim 110 \text{ \AA}$ although it leads to a most probable value of R_g , 55.17 \AA while $f=0.3$ leads to 65.58 \AA . This infers that using $f=0.1$ is also an option for SES dynamics.

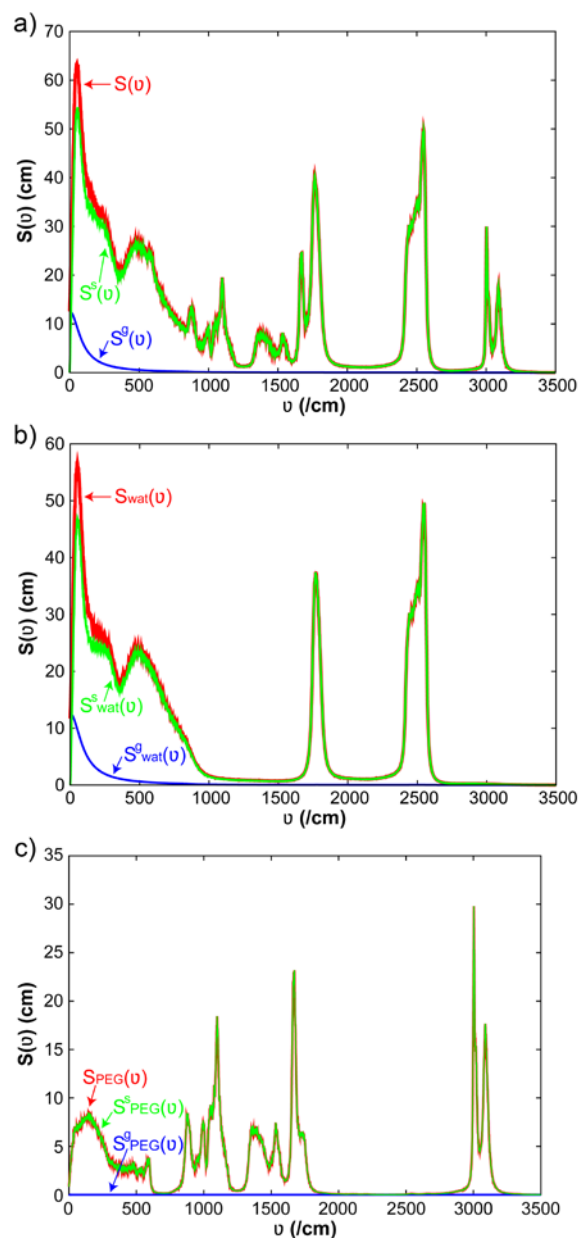


Figure S10. Starting with the PEG chain having $R_g=34.86 \text{ \AA}$, density of states (DoS) from the Fourier transform of the velocity autocorrelation function by the 2PT analysis at 300 K for the 25 wt% PEG aqueous solution

a) Total DoS $S(v)$ and the gas-like $S^g(v)$ and solid-like $S^s(v)$ components.

b) DoS of water $S_{\text{wat}}(v)$ and gas-like $S^g_{\text{wat}}(v)$ and solid-like $S^s_{\text{wat}}(v)$ components.

c) DoS of PEG $S_{\text{PEG}}(v)$ and gas-like $S^g_{\text{PEG}}(v)$ and solid-like $S^s_{\text{PEG}}(v)$ components. Most diffusional contribution is from the water dynamics.

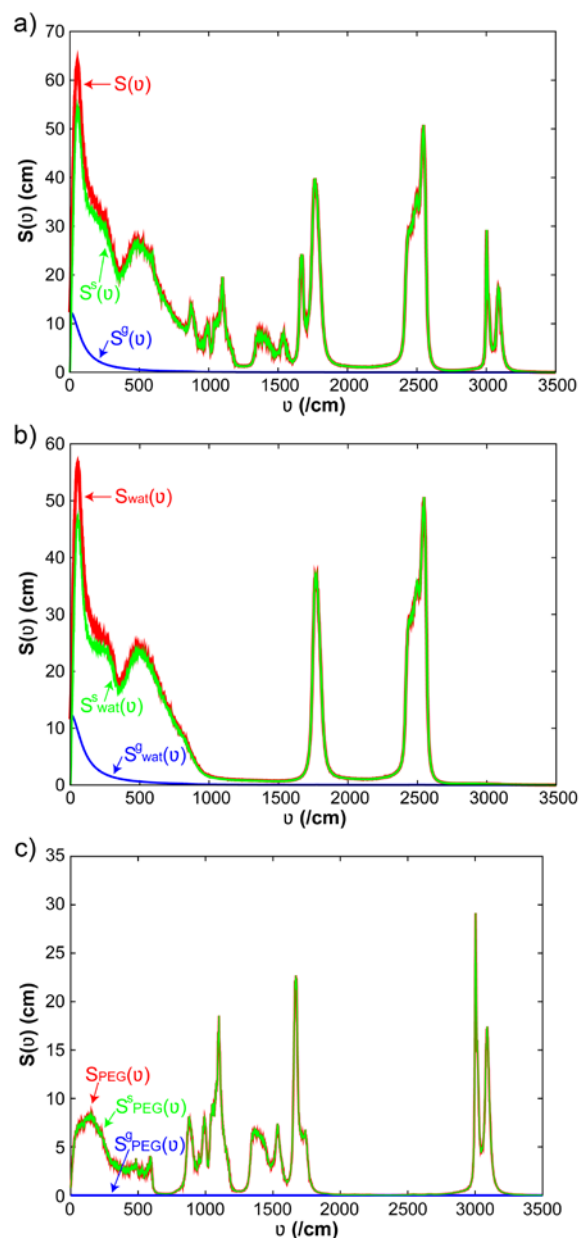


Figure S11. Starting with the PEG chain having $R_g=55.67 \text{ \AA}$, density of states (DoS) from the Fourier transform of the velocity autocorrelation function by the 2PT analysis at 300 K for the 25 wt% PEG aqueous solution

a) Total DoS $S(v)$ and the gas-like $S^g(v)$ and solid-like $S^s(v)$ components.

b) DoS of water $S_{\text{wat}}(v)$ and gas-like $S^g_{\text{wat}}(v)$ and solid-like $S^s_{\text{wat}}(v)$ components.

c) DoS of PEG $S_{\text{PEG}}(v)$ and gas-like $S^g_{\text{PEG}}(v)$ and solid-like $S^s_{\text{PEG}}(v)$ components. Most diffusional contribution is from the water dynamics.

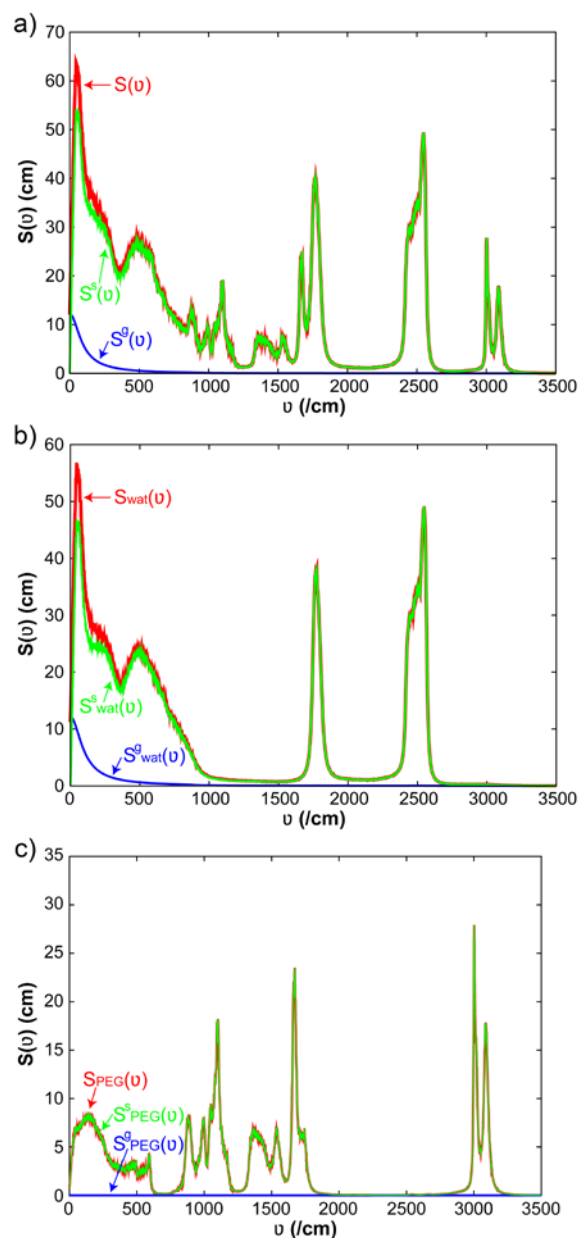


Figure S12. Starting with the PEG chain having $R_g=78.77 \text{ \AA}$, density of states (DoS) from the Fourier transform of the velocity autocorrelation function by the 2PT analysis at 300 K for the 25 wt% PEG aqueous solution

a) Total DoS $S(v)$ and the gas-like $S^g(v)$ and solid-like $S^s(v)$ components.

b) DoS of water $S_{\text{wat}}(v)$ and gas-like $S^g_{\text{wat}}(v)$ and solid-like $S^s_{\text{wat}}(v)$ components.

c) DoS of PEG $S_{\text{PEG}}(v)$ and gas-like $S^g_{\text{PEG}}(v)$ and solid-like $S^s_{\text{PEG}}(v)$ components. Most diffusional contribution is from the water dynamics.